


Article

Design and Experiment of Nondestructive Post-Harvest Device for Tomatoes

Linlu Zu ^{1,2} , Mingzheng Han ³, Jiuqin Liu ¹, Pingzeng Liu ^{2,3}, Tianhua Li ¹ and Fei Su ^{1,*}

¹ College of Mechanical and Electronic Engineering, Shandong Agricultural University, Tai'an 271018, China
² Key Laboratory of Huang-Huai-Hai Smart Agricultural Technology, Ministry of Agriculture and Rural Affairs, Tai'an 271018, China
³ College of Information Science and Engineering, Shandong Agricultural University, Tai'an 271018, China
* Correspondence: sufei@sdau.edu.cn

Abstract: This paper proposed a whole process tomato harvester with a nondestructive post-harvest collection operation mode, which was aimed to solve the high damage rate problem during the automatic greenhouse tomato harvesting process. The post-harvest device mainly included the net bag mechanism, the conveying and collecting mechanism, whose structure and materials were carefully designed to satisfy the nondestructive collection principle. Numerical simulation was done to evaluate the damage under three working conditions, which showed that the peak contact stress of tomatoes was 0.107 MPa, 0.098 MPa, and 0.11 MPa, respectively, all smaller than the damage stress of tomato peel tissue. In the postharvest prototype experiment, the degree of mechanical damage based on the shelf life of tomatoes during the color turning stage and red ripening stage was used as the evaluation index. Results showed that when tomatoes were dropped from the 60 mm higher position than the net bag mechanism, and the speed of the conveyor belt was 9 r min^{-1} , the degree of mechanical damage at the color turning stage and red ripening stage was 1.9% and 9.5%, respectively. The harvest time of greenhouse tomatoes was always around the color turning stage, thus the proposed device can well meet the agricultural requirements.



Citation: Zu, L.; Han, M.; Liu, J.; Liu, P.; Li, T.; Su, F. Design and Experiment of Nondestructive Post-Harvest Device for Tomatoes. *Agriculture* **2022**, *12*, 1233. <https://doi.org/10.3390/agriculture12081233>

Academic Editor: Jin He

Received: 20 July 2022

Accepted: 14 August 2022

Published: 16 August 2022

Publisher's Note: MDPI stays neutral with regard to jurisdictional claims in published maps and institutional affiliations.



Copyright: © 2022 by the authors. Licensee MDPI, Basel, Switzerland. This article is an open access article distributed under the terms and conditions of the Creative Commons Attribution (CC BY) license (<https://creativecommons.org/licenses/by/4.0/>).

Keywords: nondestructive collection; tomato; numerical simulation; shelf life; damage rate

1. Introduction

Tomato is one of the most extensively used fruit or vegetable crops in the world, with approximately 180 million tons of tomato fruits produced one year since 2016 [1,2], thus developing harvesting machinery instead of human labor is the future development direction [3–5]. However, there are a lot of mechanical operations in the whole harvesting process, which is easy to damage the tomato fruit, thereby reducing the nutrition and storability, and affecting the subsequent quality grading, processing, and sales [6–8]. Therefore, the fruit damage problem must be a focus when developing a tomato harvester.

Current studies correlated with nondestructive picking of fruits and vegetables [9,10] were mainly focused on the design of the end effector. Chen et al. [11] developed a pneumatic sucking-gripping integrated non-destructive end-effector for tomatoes and proposed a non-destructive control method, where the direct damage rate during tomato picking is 2.58% and 72 h browning rate is 1.76%. Ling et al. [12] developed a four fingered dexterous hand with the goal of not excessively damaging tomato fruits and plants, which could complete picking by applying tension to tomatoes through vacuum suction cups and four fingers. Xu et al. [13] designed a double v-finger navel orange end effector, which achieved stable blessing by pasting buffer material on the surface of the pressure sensor on the v-finger and combining the force feedback system, and the navel orange damage rate was 0 during picking. Miao et al. [14] designed a compliant mechanism and studied the compliant constant force characteristics in order to reduce the damage caused by clamping apples using an end effector, with the damage rate of apples lowered to 5%. In addition,

there are soft manipulators for nondestructive picking of citrus, strawberry, brown gourd, and spherical fruit [15,16].

In order to realize the nondestructive picking of slender fruits and vegetables, Jia et al. [17] proposed a soft pneumatic gripper with aeration and spiral motion, based on the finite element static simulation analysis of the gripper, studied the interaction effect of each factor on the spiral characteristics of the soft pneumatic gripper by using the three-factor and three-level central combination design and response surface analysis method. Fan et al. [18] planned the grasping positions of a three-finger end-effector in two cases to determine an optimal three-finger grip posture in order to improve picking efficiency and reduce damage, and found that the rotation–horizontal pull pattern with the combination of horizontal displacement and rotation angle yields the minimum separation force for apple picking through ABAQUS simulation software and the response surface analysis method, and the test results showed that the average three-finger grip force required for rotary tug-pull picking was 10.33 N which can reduce damage to the apple. Hou et al. [19] proposed the soft grasping mechanism of human fingers for tomato-picking bionic robots, scanned the hand to obtain the internal structure of fingers by a computerized tomography scanner, and defined the soft contact mechanical index for characterizing the degree of softness of a finger region during gentle grasping, so as to maximize the protection of the fruit.

At the same time, related research on the new generation of ‘soft grip’ robots have been carried out which are used for harvesting soft textured fruits, such as Belgium’s Soft Robotics group developed the flexible composite humanoid robot hand, Panasonic’s tomato harvesting robot, Agrobot’s strawberries picking robot, Ridder developed a multifunctional tomato harvesting robot named “GRoW” [20]. Specifically speaking, Zha et al. [19] used finite element analysis and multiple linear regression to investigate the effects of mechanics and structure of finger tissues on the soft contact mechanical index for tomato-picking bionic robots. Xiong et al. [21] presented a novel cable-driven gripper with perception capabilities for autonomous harvesting of strawberries. The gripper had the capability to store several strawberries which reduced travel time for the manipulator arm. Dimeas et al. [22] proposed a hierarchical control scheme based on a fuzzy controller for the force regulation of the gripper and proper grasping criteria for efficient strawberry harvesting.

The above studies mainly focused on the damage caused by the end effector to fruits and vegetables during picking, while there was little mention of the damage during the post-harvest collection process, i.e., after fruits and vegetables were separated from the stem. In order to truly improve productivity, the mechanized harvesting process of fruits and vegetables must be realized in the whole process [23]. The so-called whole process refers to both the picking line, the post-harvest fruit and vegetable collection line, and finally, entering the market in the form of containerized fruit and vegetable products. Therefore, with the deepening of the research on the end effector, it is particularly urgent to study the damage to fruits and vegetables in the post-harvest collection process [24].

In this paper, a tomato harvester with full process operation mode was proposed, which mainly focused on analyzing the performance of the post-harvest collection device. The damage degree of tomatoes was used as the evaluation index to quantify whether the device design was reasonable or not, so as to provide a solution for reducing or even lossless collection of greenhouse tomatoes.

2. Machine Structure and Working Principle

2.1. Whole Machine Structure of the Tomato Harvester

The tomato harvester was mainly composed of a picking vehicle and a transport vehicle, mainly including a picking mechanism and a non-destructive collection device. The picking vehicles and transport vehicles completed the tasks of picking, collecting, and transporting, and realized the whole process operation. The structure of the whole machine was shown in Figure 1, and the main technical parameters were shown in Table 1.

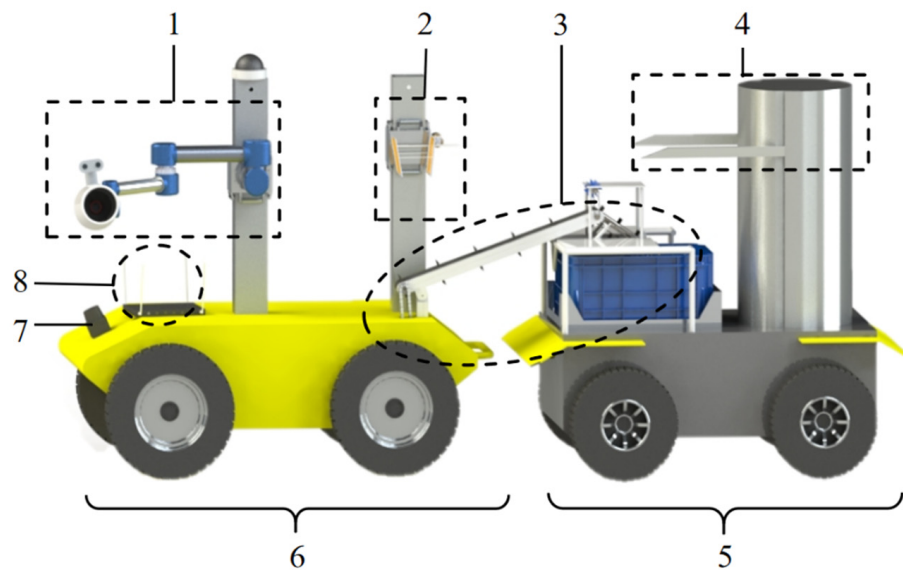


Figure 1. Whole machine structure of the tomato harvester: 1. Picking mechanism 2. Net bag mechanism 3. Conveying and collecting mechanism 4. Fork 5. Transport vehicle 6. Picking vehicle 7. Lidar module 8. Communication control module.

Table 1. Main technical parameters.

Parameter	Value
Picking vehicle length × width × height/mm	1072 × 709 × 407
Transport vehicle length × width × height/mm	884 × 561 × 407
weight/kg	80
Rated power/w	400
Running speed/(m s ⁻¹)	1~2
Endurance time/h	≥6
Picking height range/cm	46~120
Communication interface	RS232

2.2. Working Principle

The picked tomatoes finally entered the collection box through the intermediate conveying mechanism, and then the fork lifted the collection box to complete the stacking. The operation mode is shown in Figure 2, which mainly includes three working conditions. First, after picking the tomatoes, the picking robotic arm moves to the top of the net bag through the horizontal plane of its height, and then drops the tomatoes into the net bag, without having to return to the bottom of the guide rail to unload the tomatoes after picking. Then, the net bag mechanism unloads tomatoes to the conveyor belt, and finally, tomatoes enter the collection frame with the conveyor belt.

In order to lower the mechanical damage to tomatoes during the post-harvest process, the net bag was designed as a flexible net, which had an energy-absorbing and buffering effect, thus could greatly reduce the damage on the tomato surface. The roller brush on the conveyor belt could reduce the speed of tomatoes when leaving the conveyor belt and entering the collection box, which could lower the collection box's impact effect on tomatoes. When the collection box was full, the transport vehicle could separate from the picking vehicle, and the collection box was transported to the designated position in the greenhouse for packing and palletizing.

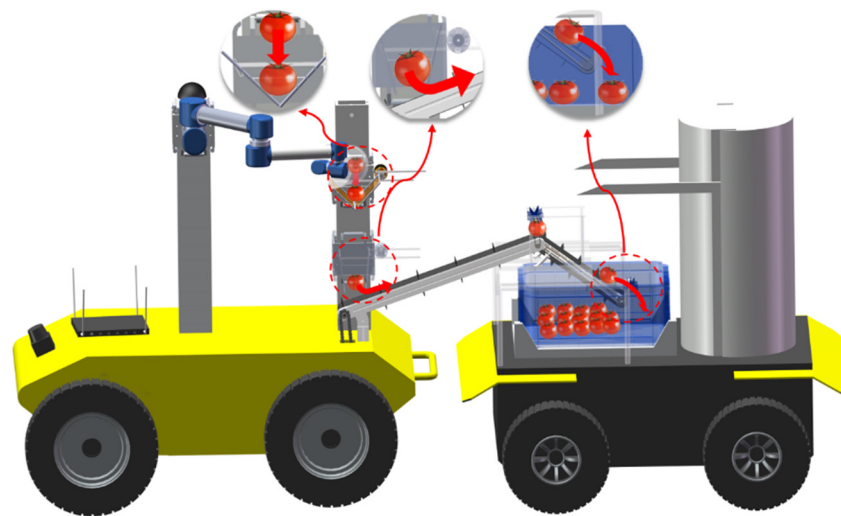


Figure 2. The moving route of tomatoes during the post-harvest process after picking.

3. Design of Non-Destructive Collection Device

3.1. Net Bag Mechanism

3.1.1. Working Principle of Net Bag Mechanism

The net bag mechanism was located on the guide rail and can move up and down, which was used to catch the tomatoes dropped by the picking robot arm, and then unloaded the tomatoes to the conveyor belt. The net bag was composed of two bilateral symmetry pieces. As shown in Figure 3a, the left and right holes on the rod cooperate to form a rotating pair. The net bag is driven by a servo motor, and the two racks mesh with the gears on the output shaft of the motor, respectively. During one rotation of the gear, the two racks move in opposite directions, driving the net bag to close. The opening and closing principle of the net bag is shown in Figure 3b. In the initial state, the net bag mechanism was V-shaped, and the picked tomatoes fall into the net bag from a certain height. The net bag was woven from flexible rubber strips, which had a good energy absorption and buffering effect. When the tomatoes were unloaded, the net bag was Λ -shaped.

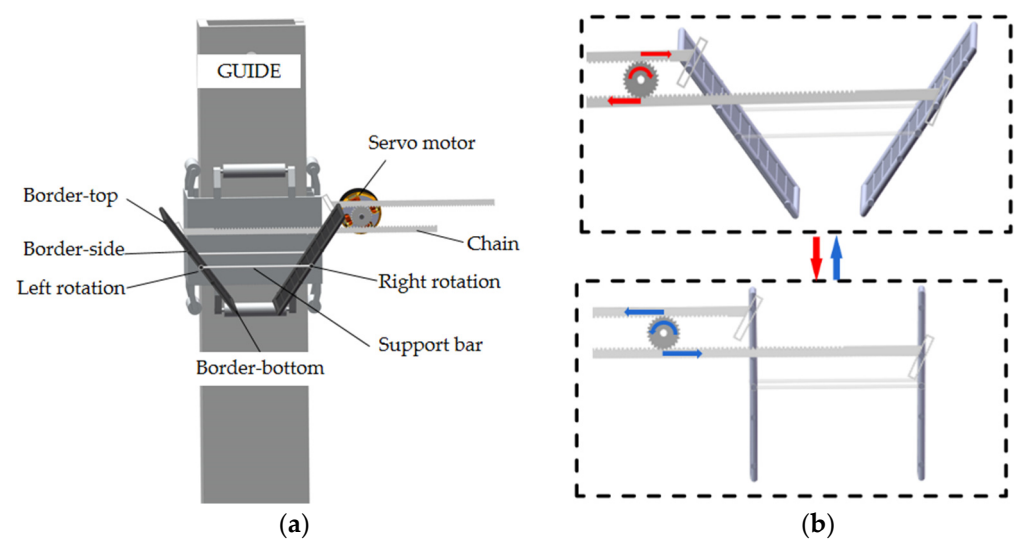


Figure 3. Structure and working principle of the net bag mechanism. (a) Structure of net bag (b) Working principle of net bag.

3.1.2. Dimension Parameter Calculation of the Net Bag Mechanism

In order to successfully complete the change process of the net bag mechanism from the “V” shape to the “Λ” shape, it was necessary to theoretically calculate the size of the mechanism. The tomato fruit was approximately regarded as a regular sphere. For most tomatoes, the maximum diameter was 85 mm and the minimum was 48 mm [25]. When the tomato falls into the net bag mechanism, two constraints should be met:

1. The tomato with the smallest diameter could not collide with the lower frame of the net bag.
2. The tomato with the largest diameter could not collide with the upper frame, and could be unloaded to the conveyor belt through the net bag smoothly.

From the geometric relationship shown in Figure 4, the following Equations were obtained:

$$\gamma = \arcsin\left(\frac{r_{\min}}{\Delta + r_{\min}}\right) \quad (1)$$

$$d = \frac{r_{\max}}{\tan[(90 - \gamma)/2]} \quad (2)$$

$$L = \frac{d}{\sin \gamma} = \frac{r_{\max}/\tan[(90 - \gamma)/2]}{\sin \gamma} \quad (3)$$

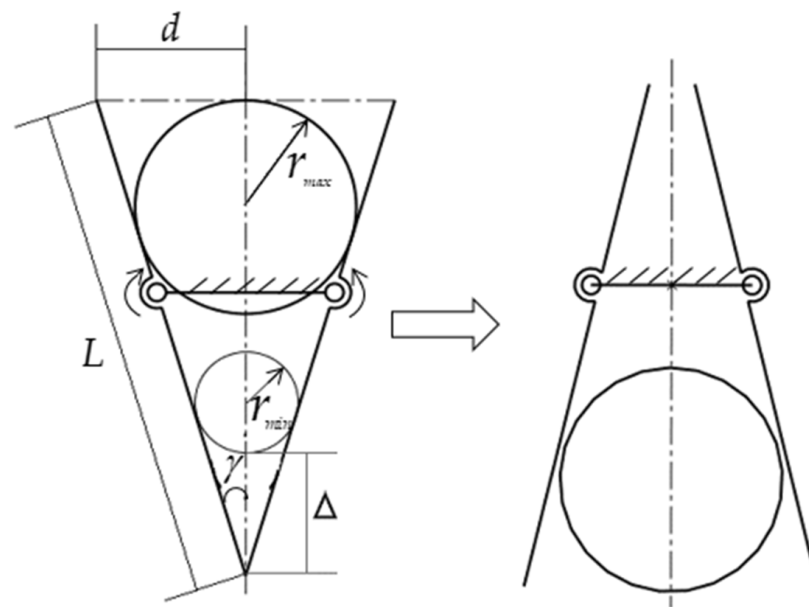


Figure 4. The tomato movement diagram in the net bag mechanism.

In Figure 4, γ is the closed half angle of the net bag, that is, one-half of the angle between the borders of the net bag; r_{\max} and r_{\min} are the maximum and minimum radius of the tomato, respectively; Δ is the reserved safety distance; d is the distance between the upper frame of the net bag and its symmetrical reference plane in the initial state; L is the length of the side frame of the net bag. The value of Δ needs to be calculated by the simulation experiment in Section 4, i.e., if $\Delta = 50$ mm, according to Equations (1)–(3), we get $\gamma = 19^\circ$, $d = 59.5$ mm, $L = 183.5$ mm.

3.1.3. The Hyperelastic Constitutive Model of Rubber Materials

The net bag was weaved by rubber strips. The rubber material was a typical nonlinear elastic material. Due to the large deformation ability, this material could recover after unloading. There exists an elastic potential energy function to describe the constitutive relationship, so it was also called super elastic material, elastic material, or Green mate-

rial [26]. This paper adopted the Mooney-Rivlin strain energy function model in the form of 2 parameters, and its expression was:

$$W = C_{01}(I_1 - 3) + C_{10}(I_2 - 3) \quad (4)$$

In the formula, I_i represents the i -th invariant of the Green strain tensor; C_{ij} represents the model material parameters.

The constitutive equation of the Hyperelastic rubber material could be expressed as of the second kind Kirchhoff stress tensor S and the Cauchy-Green strain tensor E :

$$\begin{cases} S = \frac{\partial W}{\partial E} \\ S_{ij} = \frac{\partial W}{\partial E_{ij}} = \frac{\partial W}{\partial I_1} \frac{\partial I_1}{\partial E_{ij}} + \frac{\partial W}{\partial I_2} \frac{\partial I_2}{\partial E_{ij}} + \frac{\partial W}{\partial I_3} \frac{\partial I_3}{\partial E_{ij}} \end{cases} \quad (5)$$

According to Equations (4) and (5), and combined with the relevant nonlinear continuum theory, it could be deduced that the functional relationship between engineering stress and engineering strain under uniaxial tension was:

$$\sigma = 2[(1 + \varepsilon) - (1 + \varepsilon)^{-2}] [C_{01} + (1 + \varepsilon)^{-1} C_{10}] \quad (6)$$

The above equation was the Mooney-Rivlin constitutive model of rubber. The model parameters can be determined by fitting the uniaxial tensile test data of the rubber material with Equation (6). In this paper, the density of silicone rubber material used in this paper is 1.4 g cm^{-3} , and the model parameters determined by the uniaxial tensile test data of silicone rubber are

$$C_{01} = -42.08, \quad C_{10} = 56.97 \text{ MPa} \quad (7)$$

3.2. The Conveying and Collecting Mechanism

As shown in Figure 5, since tomatoes are soft and easily damaged by impact, the cylinder used to lift the swing conveyor must be positioned accurately and run stably. The electric cylinder meets the requirements and is suitable for driving the swing conveyor [27]. A roller brush was designed at the end of the conveyor belt to reduce damage, where the soft brush could hinder the tomatoes to enter the collection box, so that the tomatoes could enter at a slower speed, reducing the collision between tomatoes and the collection box.

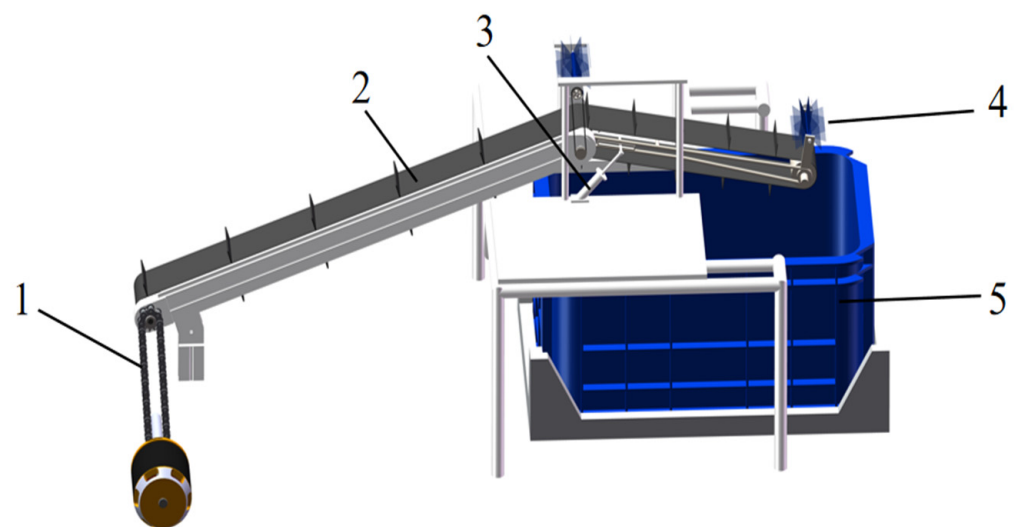


Figure 5. The conveying and collecting mechanism. 1. Roller drive source 2. Conveyor belt 3. Electric cylinder 4. Roller brush 5. Collection box.

4. Simulation Experiment of Tomato Mechanical Damage under Different Working Conditions

When the proposed collection device was working, tomatoes will have drop and collision behavior under three working conditions shown in Figure 2. Thus, potential damage may occur, so it was necessary to assess the tomato's mechanical damage by simulation. Current tomato mechanical damage degree evaluation methods include: establishing a statistical model with impact energy or peak contact force as the main independent variable, and incorporating factors such as fruit maturity and impact position into a regression equation to establish a relationship with the damage [28]; or through the finite element method [29,30] to analyze the maximum principal stress on the fruit tissue, when the maximum von Mises stress is less than its compressive failure stress, the tomato peel tissue will not rupture, and when it is greater than the failure stress, cracks begin to appear, and the crack gradually propagates along any path with increasing pressure. In this paper, the finite element simulation experiment was done with two purposes: (1) through the simulation the stress distribution of tomato can be obtained, thus, to evaluate the damage degree of the tomato during the drop and collision processes, and to preliminarily verify the rationality of the proposed design. (2) guide the optimization for the proposed net bag mechanism parameters.

4.1. Simulation Environment Construction

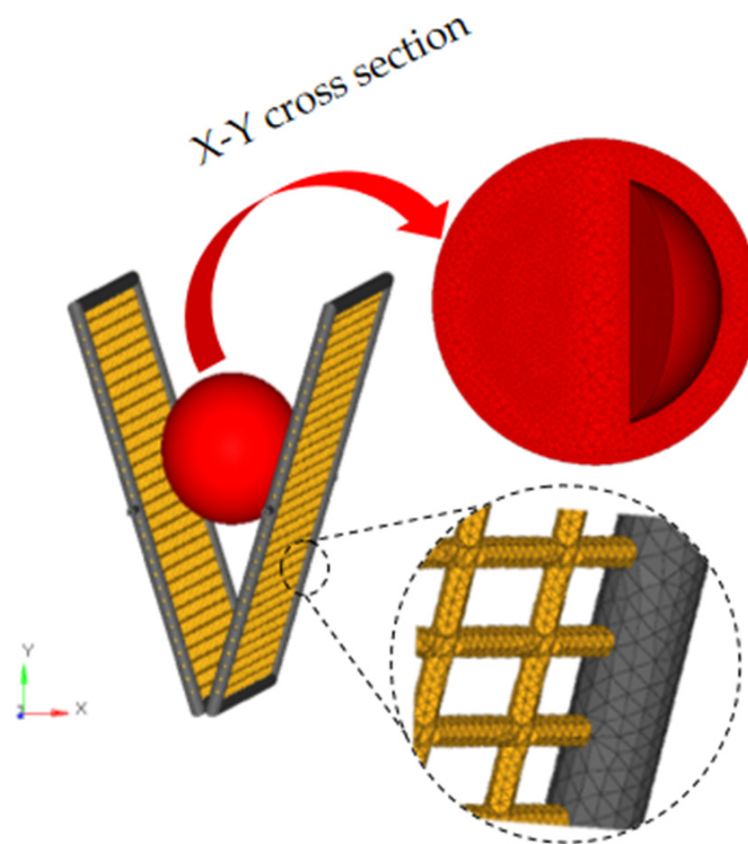
The pre-processing operations such as material setting and mesh editing are performed in the Ansys software. The output K file was solved and calculated by the nonlinear finite element analysis program LS-DYNA, and the calculation results were post-processed by LS-PrePost. The working condition of the non-destructive collection device was further simplified, with the diameter of the tomato fixed at 66.5 mm, and the solution environment under different working conditions were set as follows:

- Condition 1: Tomato falls into the net bag

In the actual working condition, the end effector of the robotic arm drops the tomato at a distance of 60 mm from the crossbar without initial speed, and then the tomato falls into the net bag. In this simulation, the air resistance was not considered. In order to reduce the calculation time, the tomato was moved 40 mm in the negative direction of the y-axis in advance, and then calculated the corresponding initial velocity according to $v = \sqrt{2gh}$, where the acceleration of gravity is set to $g = 9806.6 \text{ mm/s}^2$. Add a fixed constraint to the frame, set the mesh and the frame as bound contact, the tomato, and the mesh as "surface to surface" sliding contact, the static friction coefficient is 0.2, and the kinetic friction coefficient is 0.1. The tomato was regarded as an isotropic homogeneous elastic material. According to the rubber material data obtained in Section 3.1.3 and the data measured by related tomato mechanical tests [31,32], the material parameters were set as shown in Table 2, and the material parameters refer to the ANSYS Workbench material library. All models were divided into tetrahedral elements. The mesh size of the tomato was set to 1.2 mm, so the division has 299,402 elements and 62,472 nodes. In order to facilitate the solution, the model of the net bag device was simplified, the support rod was removed, and only the net and frame were retained. The mesh size of the mesh and the frame were both 1 mm, resulting in 769,101 elements and 200,763 nodes. The working condition 1 and the meshing of the model in the simulation environment were shown in Figure 6.

Table 2. Material parameter setting.

Parameter	Value
Tomato density/(g cm ⁻³)	0.99
Tomato elastic modulus/MPa	0.66
Poisson's ratio of tomato	0.37
Tomato Yield Stress/MPa	0.122
Silicone rubber density/(g cm ⁻³)	1.4
Silicone rubber material parameter C10/MPa	-42.38
Silicone rubber material parameter C01/MPa	56.97
Net bag border density/(g cm ⁻³)	2.7
Net bag frame elastic modulus/MPa	70,000
Net bag border Poisson's ratio	0.33

**Figure 6.** Condition 1 and model meshing in the simulation environment.

- Condition 2: Tomatoes are put on the conveyor belt by the net bag

The simplified case of working condition 2 in the simulation environment is shown in Figure 7. The tomato was released 10 mm away from the conveyor belt without initial speed, the conveyor belt is simplified to a module composed of only two adjacent baffles, and the conveyor belt inclination angle was 20°. The left and right sections of the conveyor belt were set as fixed constraints, and the tomato had no initial velocity release. The conveyor belt was made of PVC material with a density of 1.37 g cm⁻³, an elastic modulus of 2700 MPa, and a Poisson's ratio of 0.4. All model mesh sizes were 1.2 mm.

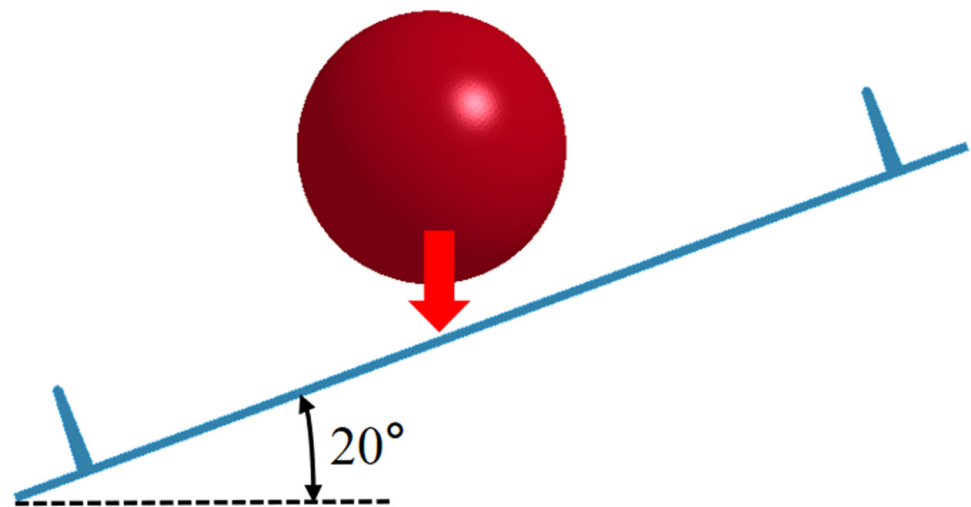


Figure 7. Condition 2 in the simulation environment.

- Condition 3: Tomatoes enter the collection box from the conveyor belt

The simplified situation of working condition 3 in the simulation environment is shown in Figure 8. The conveyor belt rotated clockwise at 8.6 r min^{-1} . The center of the conveyor roller was 59 mm from the bottom surface of the collection frame. The tomatoes entered the collection frame with the rotation of the roller. The front and rear sections and the left section of the collection frame were set as fixed constraints. The material parameters of the tomato and collection box were the same as the previous ones. Considering the computer performance and weighing the calculation accuracy and efficiency, the meshing method in case 2 was automatic, the tomato model used tetrahedral elements, the conveyor belt model and the collection box model were hexahedral elements, and a total of 9570 nodes and 22,907 elements were generated, performed the mesh quality check function, and got an average mesh quality of 0.8.

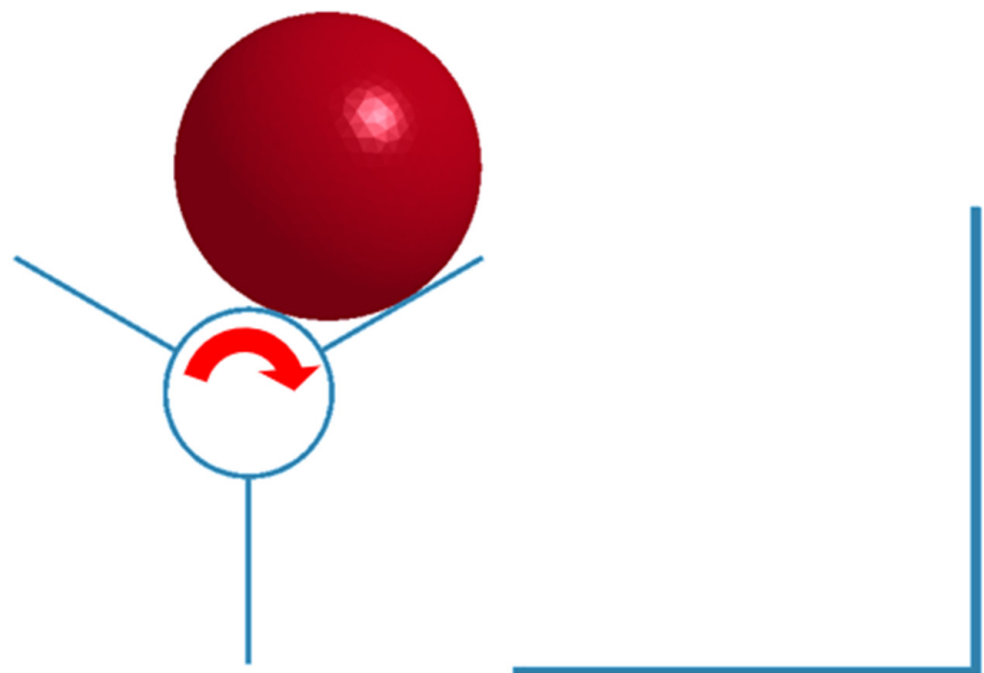


Figure 8. Condition 3 in the simulation environment.

4.2. Simulation Results

For working condition 1, as shown in Figure 9 the peak contact stress during the tomato falling process is 0.107 MPa, and the falling displacement is 33 mm. Since the peak contact stress was less than the damage stress of tomato peel tissue by 0.122 MPa, thus the tomato peel could not be damaged, and the design of the net bag device was reasonable. The stress inside the tomato peel is all less than 0.107 MPa, thus even the tomato partition more sensitive to bruising could also not be damaged. When the tomato was moved to a distance of 42 mm from the lower border, the speed was reduced to 0, and it no longer moved in the negative direction of the y-axis. The tomato did not collide with the lower border, indicating that the anti-collision safety 50 mm margin Δ in Formulas (1)–(3) met the constraints, thus providing calculation basis for the dimension parameter of the net bag mechanism in Section 3.1.2.

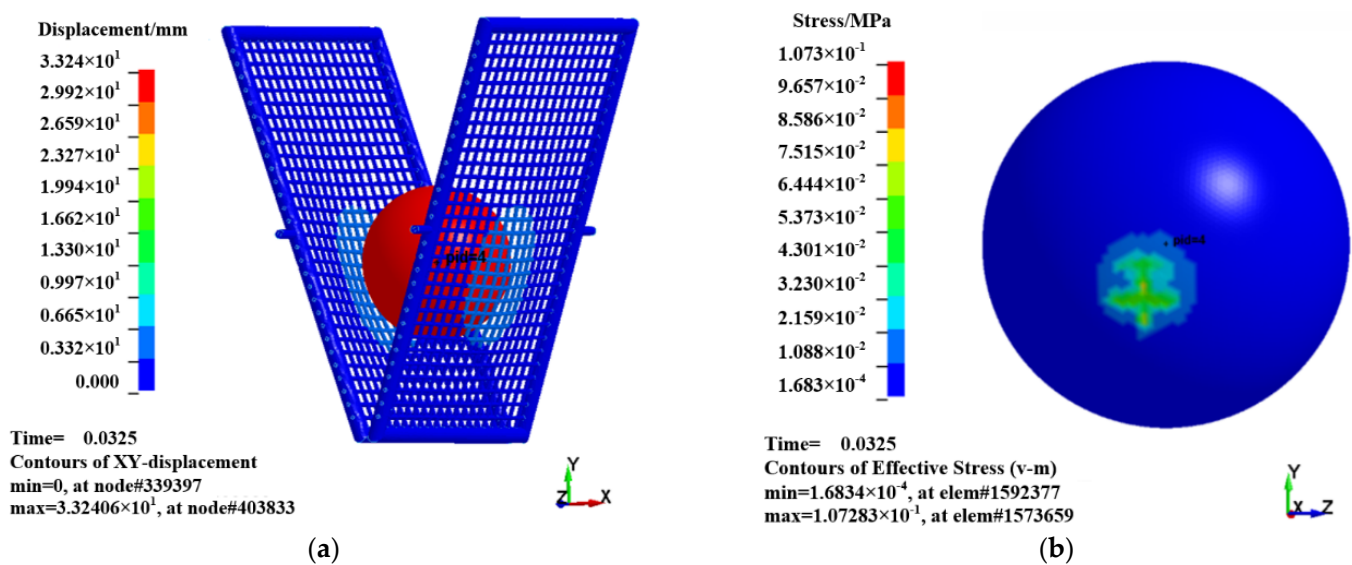


Figure 9. Simulation results of tomato drop in condition 1. (a) The falling displacement of the tomato (b) The maximum stress on the tomato.

For working condition 2 and working condition 3, the simulation results were shown in Figures 10 and 11, and the peak contact stress of tomato was 0.098 MPa and 0.121 MPa, respectively. In condition 3, the peak stress of the tomato was too close to its yield stress, so the PVC material of the collection box was changed to corrugated paper, the thickness is 3 mm, and the material property was set as orthotropic. The peak contact stress of tomato was reduced to 0.11 MP, and the damage reduction effect of corrugated paper was more significant than that of PVC, thus providing an optimized selection basis for the material of the collection box.

4.3. Comparison of Energy Absorption Effect of the Net Bag Mechanism

If the net bag mechanism was not used, the tomato was dropped from a distance of 60 mm from the conveyor belt, and then collided with the conveyor belt. At this time, the peak contact stress is shown in Figure 12, reaching 0.126 MPa, exceeding its yield stress limit, so the tomato will be biological deformation, and the peel tissue may be damaged.

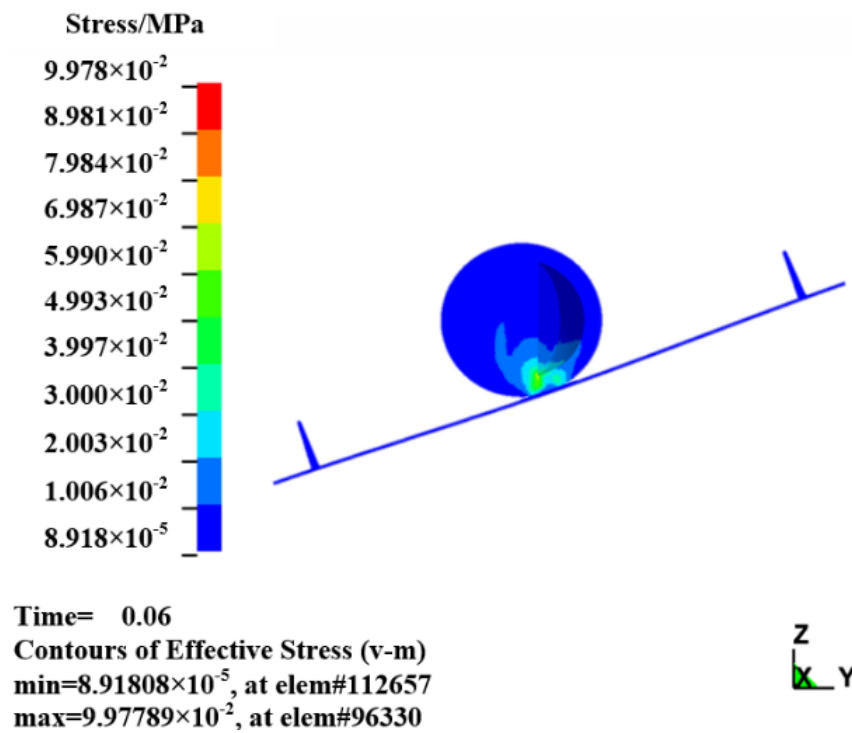


Figure 10. Simulation results of tomato drop in condition 2.

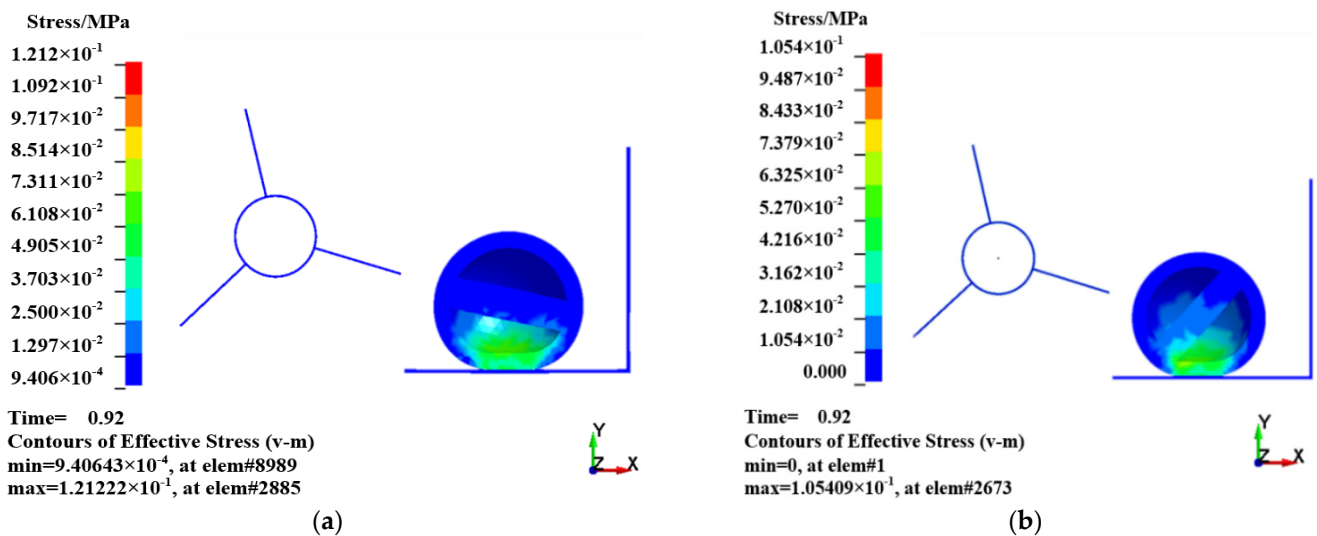


Figure 11. Simulation results of tomato drop in condition 3 with (a) PVC material and (b) Corrugated paper material.

The internal energy of the tomato during the drop and collision process was compared with that in working condition 1. The results are shown in Figure 12c, when the net bag mechanism is used, the peak internal energy of the tomato is 17.5×10^{-3} J. However, when the net bag is not used, the peak internal energy is 63.4×10^{-3} J. So, the peak internal energy was reduced to 45.9×10^{-3} J by the net bag mechanism, indicating that the peak energy absorption rate of the net bag reaches 72.4%, which could obviously be used as a buffer component in the post-harvest collection process.

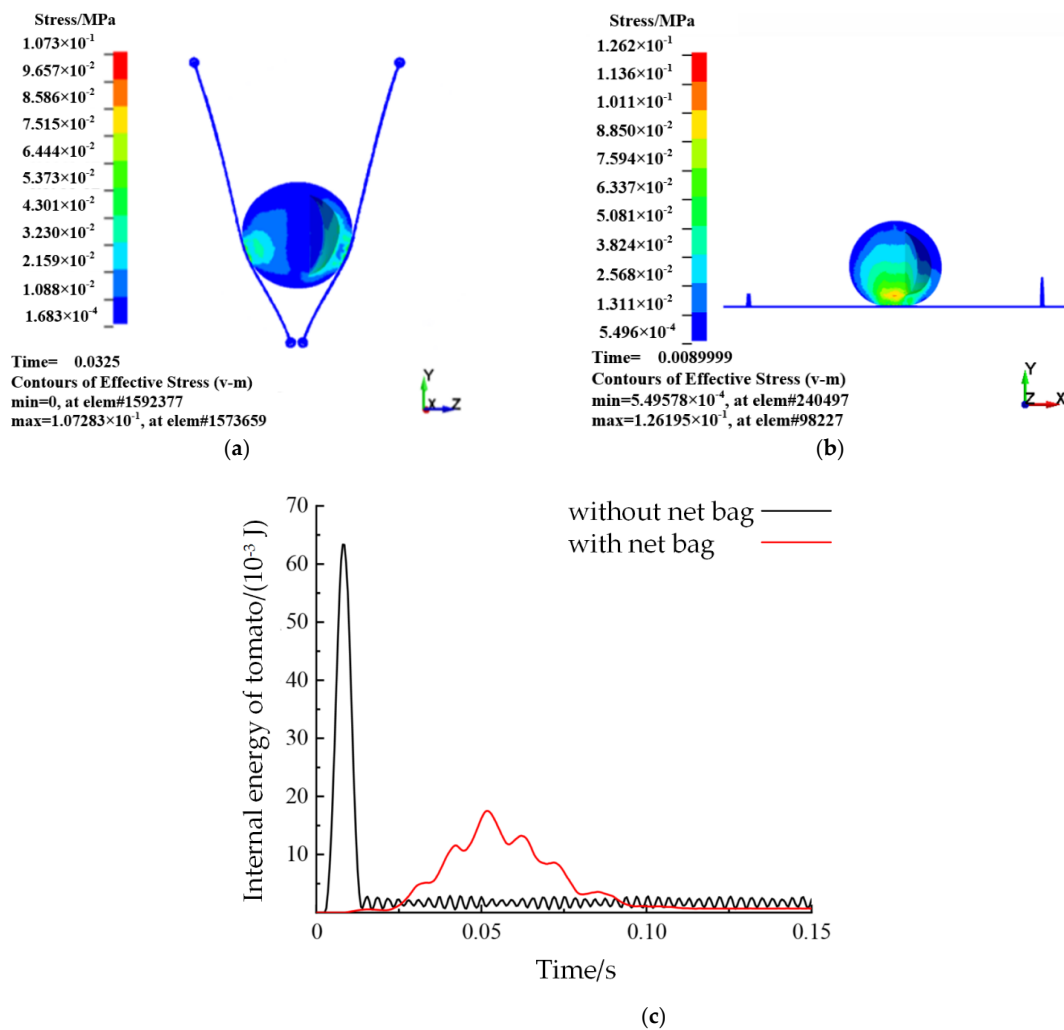


Figure 12. Comparison of the energy absorption effect (a) with and without (b) the net bag mechanism. (c) Comparison of internal energy of tomato when the drop height is 60 mm.

5. Test of the Post-Harvest Prototype

5.1. Test Conditions

The tomatoes used in the test were taken from the tomato solar greenhouse of Shandong Agricultural University. The tomato variety tested was “Sheng Luo Lan 3689”, of which 100 tomatoes were in the turning stage and 100 tomatoes were in the red ripening stage. Tomatoes at the turning stage and red ripening stage were randomly divided into 5 groups, with 20 samples in each group. One group was used as the control group to determine the normal shelf life, and the other four groups were used as the test group. The post-harvest prototype is shown in Figure 13, and the relevant test parameters are shown in Table 3.

Table 3. Test parameters.

Parameter	Value
Tomato number/pc	200
Tomato diameter/mm	66.5 ± 3
Conveyor speed/(r min ⁻¹)	9
Corrugated paper thickness/mm	3
Room temperature/°C	20 ± 5



Figure 13. Prototype test of post-harvest collection device.

5.2. Test Method

During the test, the human hand was used to simulate the mechanical manipulator, and each tomato was released once at a distance of 60 mm from the support rod of the net bag mechanism without initial speed. This process belongs to working condition 1. The schematic diagram of the net bag mechanism test platform is shown in Figure 14. The pressure sensor (The model is RP-C7.6-ST-LF2, the trigger force is 2 g) was placed on the surface of the lower frame to detect whether the tomato collides with the lower border. The data display terminal was the laptop display screen, and the value of the pressure sensor was displayed in real time through the serial port debugging assistant. After the tomato enters the net bag, the net bag was manually controlled to reach the fruit unloading state, which belonged to working condition 2. In the subsequent process, no human was involved, the conveyor belt carried the tomatoes into the collection box which was covered with corrugated paper at the bottom, and the tomatoes left from the conveyor belt and collided with the corrugated paper. Finally, the tomato was taken out and kept indoors, observe and record whether the tomato surface was wrinkled, browned, or even mildewed every 0.5 days. When the above phenomenon occurs, recorded the number of days at this time as the shelf life. The degree of mechanical damage to tomatoes based on shelf life [33] was calculated as follows:

$$\eta = \frac{t_a - t_b}{t_a} \times 100\% \quad (8)$$

where t_a represents the shelf life of the tomatoes in the control group at different maturity stages, and t_b represents the shelf life of the tomato in the test group at different maturity stages [34].

5.3. Test Results

The shelf life was taken as the average value of the tomatoes in each group. For the control group, the shelf life of the tomato at the turning stage was 16 days at room temperature, and the shelf life of the tomato at the red ripening stage was 5.5 days. The surface of some tomatoes at the turning stage was bruised, but the peel was not broken, and the surface of some tomatoes at the red ripening stage had bruising and indentation, as shown in Figure 15. The statistics results of the shelf life for these experimental groups are shown in Figure 16, where the average shelf life of the tomatoes at the turning stage with the net bag is 15.7 days, so the average damage rate is about 1.9%; the average shelf life of the tomatoes at the red ripening stage is 4.98 days, so the average degree of mechanical

damage is 9.5%. Contrastively, when without the net bag, the average shelf life at the turning stage and the red ripening stage, respectively, are 14.7 days and 3.74 days. From the different test results between with the net bag and without the net bag, we can illustrate the actual damage reduction effect of the device. Considering that the tomato picking was generally at or before the turning period, the proposed post-harvest design prototype could meet the agronomic requirements for post-harvest tomato collection in the greenhouse.

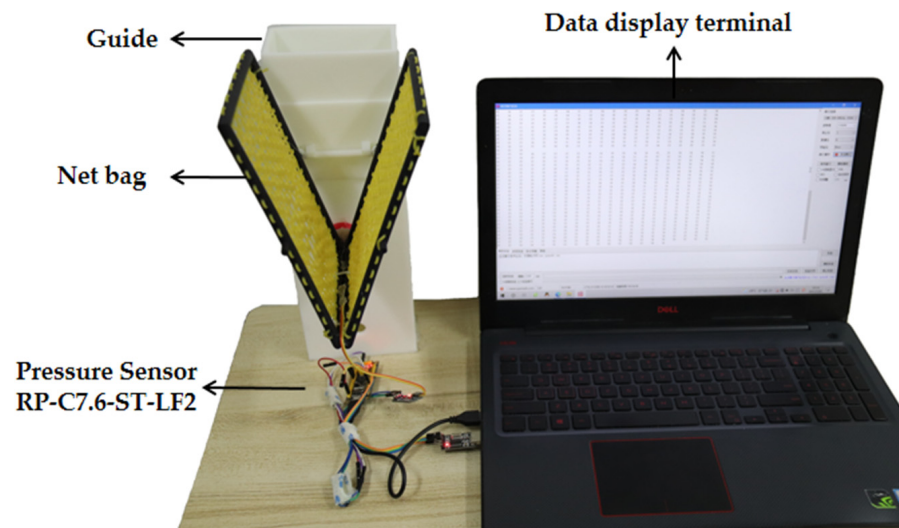


Figure 14. Test platform of the net bag mechanism.

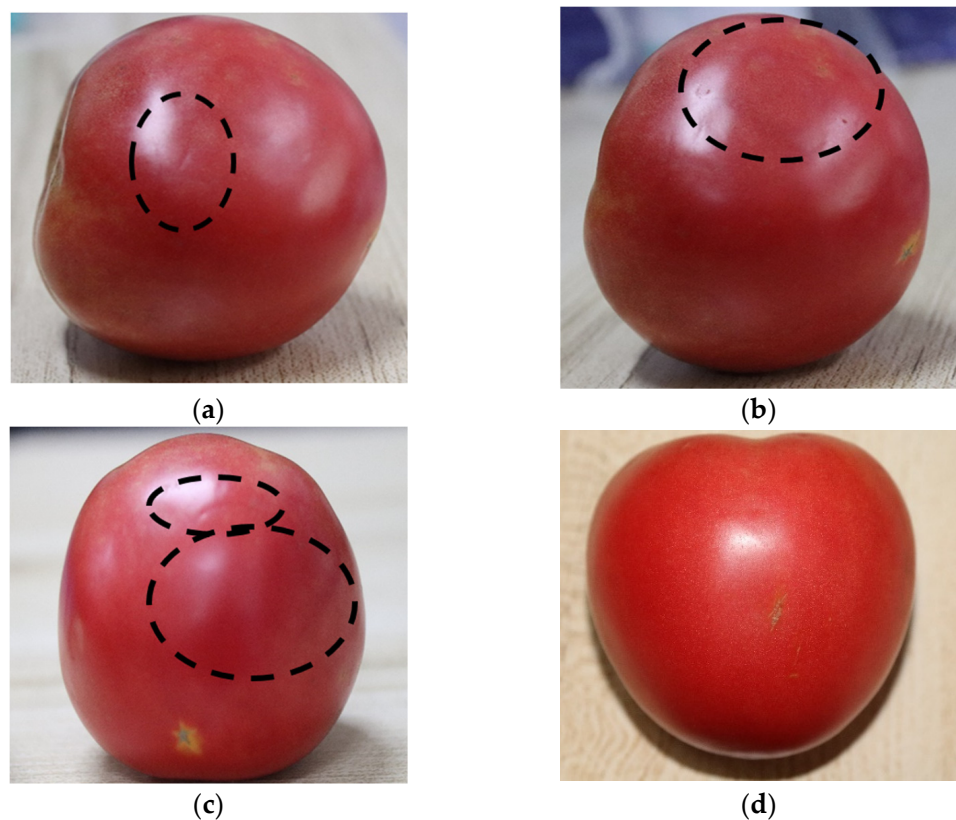
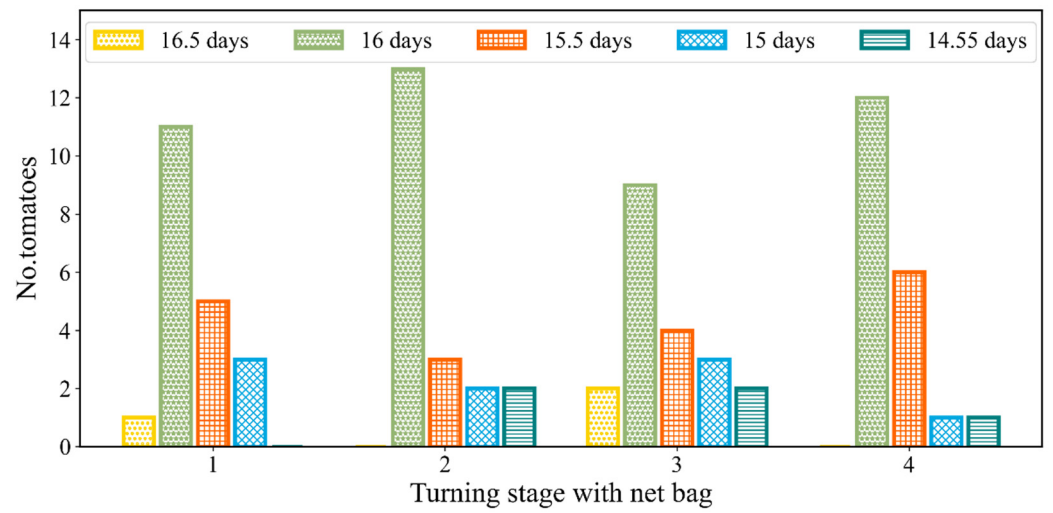
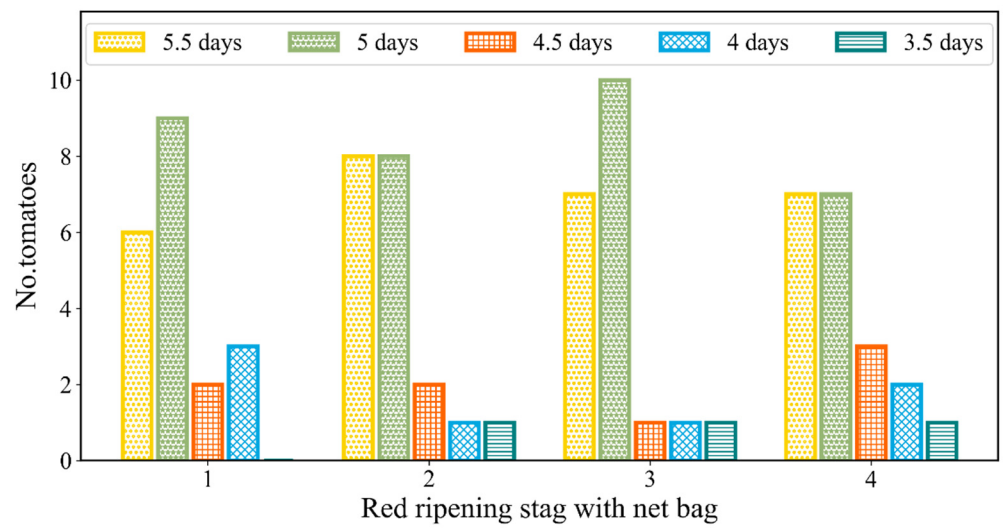


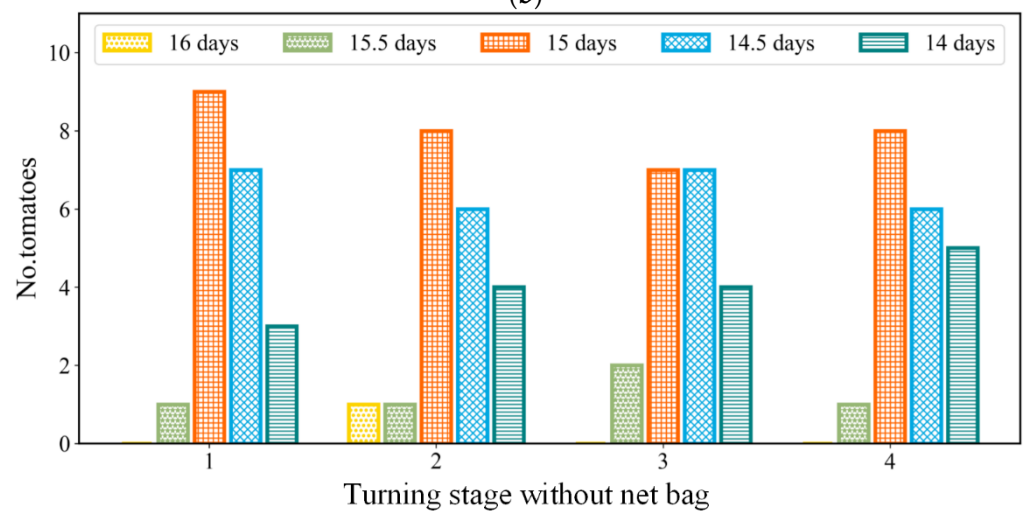
Figure 15. Tomato damage conditions (a) Indentation, (b) Bruises, (c) Indentation and Bruises, and (d) Normal ripe tomato.



(a)



(b)



(c)

Figure 16. Cont.

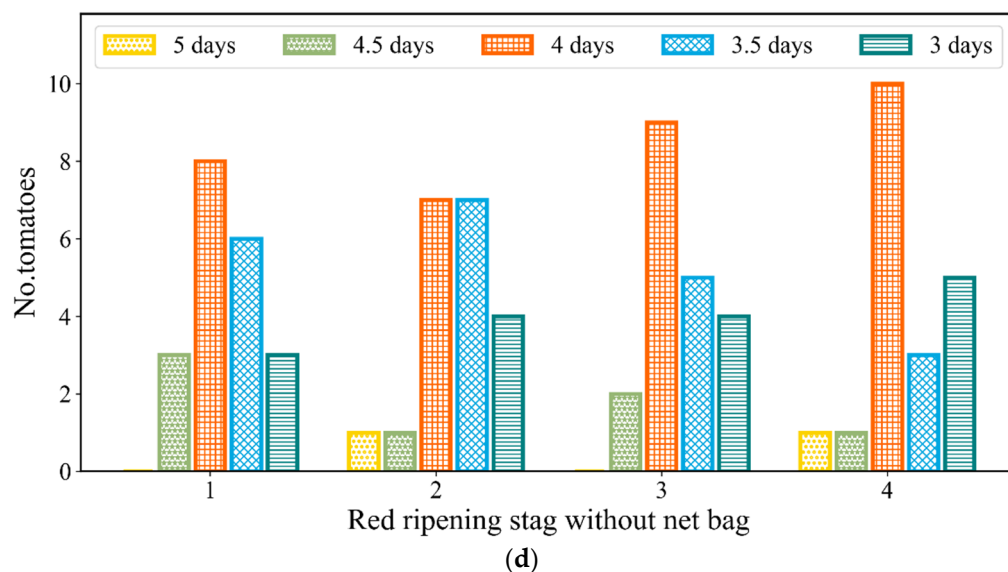


Figure 16. The statistical results of tomatoes shelf-life: (a) Turning stage with net bag; (b) Red ripening stag with net bag; (c) Turning stage without net bag; (d) Red ripening stag without net bag.

6. Discussion

This study proposed a whole process tomato harvester with a nondestructive post-harvest collection operation mode to minimize the damage to tomatoes. Through numerical simulation, the internal stress distribution of tomatoes can be known, and the structural optimization design of the postharvest collection device can also be carried out with the stress result as the target quantity. Combined with existing studies, the working effect of the device can be determined, and a design scheme can be provided for the non-destructive harvesting of tomato harvesting equipment. Table 4 shows a detailed comparison with existing studies about non-destructive harvesting and transportation.

Table 4. Scientific studies in tomato nondestructive picking.

Source	Method	Reported Metrics
Chen et al. [11]	A pneumatic sucking-gripping integrated non-destructive end-effector	Damage rate during tomato picking is 2.58%
Miao et al. [14]	Designed a compliant mechanism and studied the compliant constant force characteristics	Damage rate of apples lowered to 5%
Wang et al. [35]	Conveyer belt type packing scheme and rotary separation type packing scheme	The average damage rate during the fall is 5.05%
Shan et al. [36]	Hand-arm cooperative damage-free harvesting system	The average harvest time is 18.93 s and average shatter is 0.3 out of 18
Zhou et al. [37]	Flexible end-effector designed by genetic algorithm according to the physical characteristics of tomatoes and simulation results	Tomatoes would be successfully clamped by the end-effector with the inflation pressure less than the optimized inflation pressure
Byshov et al. [38]	Increase contact area of the fruit and container and reduce the space for the free movement of products	The maximum speed of the proposed vehicle is 1.2–1.22 times greater than the base variant trailer
Proposed	Nondestructive post-harvest collection operation mode	The degree of mechanical damage at the color turning stage is 1.9%

Through the analysis of the research status of nondestructive harvesting of soft fruits at home and abroad, most of the research focuses on the structural design and performance improvement of end-effectors, so as to reduce damage during picking, or by integrating the advantages of different structures into a specific field environment, achieve better performance through innovative optimized design. However, there are few studies about the post-harvest non-destructive collection process. This research innovatively proposes a full-process tomato harvester with a post-harvest collection operation mode. The simulation

analysis of three working conditions after tomato harvesting is carried out to confirm the mechanism feasibility. The non-destructive operation of the whole process from leaving the manipulator to entering the collection basket after the tomato picking process is realized. No research has been found on postharvest non-destructive collection devices for tomatoes, so there was some novelty in the research method.

In this paper the finite element simulation was done before the prototype test. The simulation results can make the internal mechanical damage of the tomato more intuitively understandable, and avoid some collisions in the real world. On the other hand, the simulation provides a means for the optimization of the non-destructive post-harvest structure, i.e., in this paper, the numerical simulation results of the flat net show that the peak contact stress of the tomato is 0.107 MPa, in order to further reduce tomato peak contact stress, it is necessary to increase the contact area between the net and the tomato. Thus, a feasible way is to change the plane mesh to the surface mesh. In future work, we will use the numerical simulation method to explore the functional relationship between different curvatures and the peak contact stress of the tomato, further optimize the form of the net bag, and select the most suitable curvature of the upper and lower borders.

This research made some experimental innovations, but there were still some limitations, the simulation results cannot completely predict the results of the prototype test, and the prototype test result showed that there were still a small number of tomatoes damaged, which was slightly different from the simulation result, the difference may be caused by the following reasons:

- (1) Different tomatoes had different biological parameters, resulting in different tissue mechanical properties. In addition, some tomatoes may have been infected by the flora in the natural environment, resulting in folds and mildew.
- (2) According to the stress results, the simulation test could judge whether the tomato had bio-yield deformation. When the peak stress was close to but not exceeding the yield point, a small number of cells may have ruptured. In the prototype test environment, ruptured cells would produce a series of enzymatic reactions, which would deepen the color of tomatoes and cause shrinkage, resulting in a shortened shelf life.

7. Conclusions

In this paper, a whole process tomato harvester with a nondestructive post-harvest collection operation mode was proposed. The whole working principle was first introduced, and then the structure design principle and material selection of the nondestructive post-harvest device was carried out. Finally, the post-harvest prototype was constructed and tested. The main contributions were listed as follows,

- (1) The LS-DYNA explicit dynamics solver was used to analyzing the operation effect of the post-harvest collection device. Three post-harvest working conditions were simulated to obtain the damage data to tomatoes. The simulation results showed that the post-harvest collection device would not cause mechanical damage to the tomatoes, and the relevant numerical results were important references for structural optimization.
- (2) As an energy buffering-absorbing structure, the working effect of the V-shaped rubber net bag was evaluated. Compared with the conveyor belt where the tomatoes directly collided with the PVC material, the peak internal energy of the tomatoes was reduced by 45.9×10^{-3} J, and the energy absorption rate of the rubber net bag reached 72.4%.
- (3) The prototype test results showed that the damage rate of tomatoes at the color turning stage was only 1.9%, which was almost undamaged. While the tomato at the red ripening stage reached 9.5%, that was why greenhouse tomatoes were usually not harvested at the mature stage.

Author Contributions: M.H. and J.L. designed hardware; J.L. finished hardware emulation; F.S., and T.L. analyzed the data; M.H., J.L., and L.Z. wrote the paper; F.S., L.Z. drew pictures for this paper; F.S., P.L. and T.L. reviewed and edited the paper. All authors have read and agreed to the published version of the manuscript.

Funding: This research was funded by the major science and technology innovation project of Shandong Province (NO.2019JZZY020620), and the major agricultural applied technology innovation project of Shandong province (NO.SD2019ZZ019).

Institutional Review Board Statement: Not applicable.

Informed Consent Statement: Not applicable.

Data Availability Statement: All data are presented in this article in the form of figures and tables.

Acknowledgments: The authors would like to thank the editors and all the reviewers who participated in the review.

Conflicts of Interest: The authors declare no conflict of interest.

References

1. Quinet, M.; Angosto, T.; Yuste-Lisbona, F.J.; Blanchard-Gros, R.; Bigot, S.; Martinez, J.P.; Lutts, S. Tomato Fruit Development and Metabolism. *Front. Plant Sci.* **2019**, *10*, 1554. [CrossRef] [PubMed]
2. FAOSTAT. Available online: <http://www.fao.org/faostat/en/#home> (accessed on 14 March 2022).
3. Van De Walker, B.; Byrne, B.; Near, J.; Purdie, B.; Whatman, M.; Weales, D.; Moussa, M. Developing a Realistic Simulation Environment for Robotics Harvesting Operations in a Vegetable Greenhouse. *Agronomy* **2021**, *11*, 1848. [CrossRef]
4. Idama, O.; Uguru, H. Robotization of Tomato Fruits Production to Enhance Food Security. *J. Eng. Res. Rep.* **2021**, 67–75. [CrossRef]
5. Liu, J. Research Progress Analysis of Robotic Harvesting Technologies in Greenhouse. *Trans. Chin. Soc. Agric. Mach.* **2017**, *48*, 1–18.
6. Zhang, Z.; Bian, B.; Jiang, Y. A Joint Decision-Making Approach for Tomato Picking and Distribution Considering Post-harvest Maturity. *Agronomy* **2020**, *10*, 1330. [CrossRef]
7. Hussein, Z.; Fawole, O.A.; Opara, U.L. Harvest and Post-harvest Factors Affecting Bruise Damage of Fresh Fruits. *Hortic. Plant J.* **2020**, *6*, 1–13. [CrossRef]
8. Zhu, A.; Bian, B.; Jiang, Y.; Hu, J. Integrated Tomato Picking and Distribution Scheduling Based on Maturity. *Sustainability* **2020**, *12*, 7934. [CrossRef]
9. Zhang, B.; Zhou, J.; Meng, Y.; Zhang, N.; Gu, B.; Yan, Z.; Idris, S.I. Comparative study of mechanical damage caused by a two-finger tomato gripper with different robotic grasping patterns for harvesting robots. *Biosyst. Eng.* **2018**, *171*, 245–257. [CrossRef]
10. Cao, X.; Yan, H.; Huang, Z.; Ai, S.; Xu, Y.; Fu, R.; Zou, X. A multi-objective particle swarm optimization for trajectory planning of fruit picking manipulator. *Agronomy* **2021**, *11*, 2286. [CrossRef]
11. Chen, Z.; Yang, M.; Li, Y.; Yang, L. Design and experiment of tomato picking end-effector based on non-destructive pneumatic clamping control. *Trans. CSAE* **2021**, *37*, 27–35.
12. Ling, P.P.; Ehsani, R.; Ting, K.C.; Chi, Y.T.; Ramalingam, N.; Klingman, M.H.; Draper, C. *Sensing and End-Effector for a Robotic Tomato Harvester*; ASAE: St. Joseph, MI, USA, 2004.
13. Xu, L.; Liu, X.; Zhang, K.; Xing, J.; Yuan, Q.; Chen, J.; Duan, Z.; Ma, S.; Yu, C. Design and test of end-effector for navel orange picking robot. *Trans. CSAE* **2018**, *34*, 53–61.
14. Miao, Y.; Zheng, J. Development of compliant constant-force mechanism for end effector of apple picking robot. *Trans. CSAE* **2019**, *35*, 19–25.
15. Muscato, G.; Prestifilippo, M.; Abbate, N.; Rizzuto, I. A prototype of an orange picking robot: Past history, the new robot and experimental results. *Ind. Robot. Int. J.* **2005**, *32*, 128–138. [CrossRef]
16. Peng, Y.; Liu, Y.; Yang, Y.; Yang, Y.; Liu, N.; Sun, Y. Research progress on application of soft robotic gripper in fruit and vegetable picking. *Trans. CSAE* **2018**, *34*, 11–20.
17. Jia, J.; Ye, Y.; Cheng, P.; Hu, R.; Wu, C. Design and Parameter Optimization of Soft Pneumatic Gripper for Slender Fruits and Vegetables Picking. *Trans. Chin. Soc. Agric. Mach.* **2021**, *52*, 26–34.
18. Fan, P.; Yan, B.; Wang, M.; Lei, X.; Liu, Z.; Yang, F. Three-finger grasp planning and experimental analysis of picking patterns for robotic apple harvesting. *Comput. Electron. Agric.* **2021**, *188*, 106353. [CrossRef]
19. Hou, Z.; Li, Z.; Fadji, T.; Fu, J. Soft grasping mechanism of human fingers for tomato-picking bionic robots. *Comput. Electron. Agric.* **2021**, *182*, 106010. [CrossRef]
20. Zhang, B.; Xie, Y.; Zhou, J.; Wang, K.; Zhang, Z. State-of-the-art robotic grippers, grasping and control strategies, as well as their applications in agricultural robots: A review. *Comput. Electron. Agric.* **2020**, *177*, 105694. [CrossRef]

21. Xiong, Y.; From, P.J.; Isler, V. Design and Evaluation of a Novel Cable-Driven Gripper with Perception Capabilities for Strawberry Picking Robots. In Proceedings of the IEEE International Conference on Robotics and Automation, Brisbane, Australia, 21–25 May 2018. [[CrossRef](#)]
22. Dimeas, F.; Sako, D.V.; Moulitanitis, V.C.; Aspragathos, N.A. Design and fuzzy control of a robotic gripper for efficient strawberry harvesting. *Robotica* **2015**, *33*, 1085–1098. [[CrossRef](#)]
23. Lu, W.; Wang, P.; Wang, L.; Deng, Y. Design and Experiment of Flexible Gripper for Mushroom Non-destructive Picking. *Trans. Chin. Soc. Agric. Mach.* **2020**, *51*, 28–36.
24. Liu, X.; Tian, D.; Song, M. Design and Experiment on Pneumatic Flexible Gripper for Picking Globose Fruit. *Trans. Chin. Soc. Agric. Mach.* **2021**, *52*, 30–43.
25. Ji, W.; Luo, D.; Li, J.; Yang, J.; Zhao, D. Compliance grasp force control for end-effector of fruit-vegetable picking robot. *Trans. Chin. Soc. Agric. Eng.* **2014**, *30*, 19–26.
26. Zulkifli, N.; Hashim, N.; Harith, H.H.; Shukery, M.F.M. Finite element modelling for fruit stress analysis—A review. *Trends Food Sci. Technol.* **2020**, *97*, 29–37. [[CrossRef](#)]
27. Chen, C.; Zhao, S.D.; Cui, M.; Cai, H.; Li, X. Study Status and Developing Trend of Electric Cylinder. *J. Mech. Transm.* **2015**, *39*, 181–186.
28. Van Zeebroeck, M.; Darius, P.; De Ketelaere, B.; Ramon, H.; Tijssens, E. The effect of fruit properties on the bruise susceptibility of tomatoes. *Post-Harvest. Biol. Technol.* **2007**, *45*, 168–175. [[CrossRef](#)]
29. Kabas, O.; Celik, H.K.; Ozmerzi, A.; Akinci, I. Drop test simulation of a sample tomato with finite element method. *J. Sci. Food Agric.* **2008**, *88*, 1537–1541. [[CrossRef](#)]
30. Li, Z.; Andrews, J.; Wang, Y. Mathematical modelling of mechanical damage to tomato fruits. *Post-Harvest. Biol. Technol.* **2017**, *126*, 50–56. [[CrossRef](#)]
31. Li, Z.; Li, P.; Yang, H.; Liu, J.; Xu, Y. Mechanical properties of tomato exocarp, mesocarp and locular gel tissues. *J. Food Eng.* **2012**, *111*, 82–91. [[CrossRef](#)]
32. Li, D.; Li, Z.; Tchuembou-Magaia, F. An extended finite element model for fracture mechanical response of tomato fruit. *Post-Harvest. Biol. Technol.* **2021**, *174*, 111468. [[CrossRef](#)]
33. Li, Z.G.; Li, P.P.; Liu, J.Z. Relationship between mechanical property and damage of tomato during robot harvesting. *Trans. CSAE* **2010**, *26*, 112–116.
34. Jin, S.; Ding, Z.; Xie, J. Modified Atmospheric Packaging of Fresh-Cut Amaranth (*Amaranthus tricolor* L.) for Extending Shelf Life. *Agriculture* **2021**, *11*, 1016. [[CrossRef](#)]
35. Wang, Z. *Design and Research of Automatic Conveying and Packing Machine on Kiwifruit Harvesting Robot*; Northwest Agriculture & Forestry University: Xianyang, China, 2019; Volume 5, pp. 50–58.
36. Shan, H. *Design and Experiment of Robotic Hand-Arm Cooperative Damage-Free Harvesting System for Trellis Grapes*; Jiangsu University: Zhenjiang, China, 2021; Volume 6, pp. 69–73.
37. Zhou, K.; Xia, L.; Liu, J.; Qian, M.; Pi, J. Design of a flexible end-effector based on characteristics of tomatoes. *Int. J. Agric. Biol. Eng.* **2022**, *15*, 13–24. [[CrossRef](#)]
38. Byshov, N.V.; Borychev, S.N.; Kashirin, D.E.; Kokorev, G.D.; Kostenko, M.Y.; Rembalovich, G.K.; Danilov, I.K. Theoretical studies of the damage process of easily damaged products in transport vehicle body during the on-farm transportation. *ARPN J. Eng. Appl. Sci.* **2018**, *13*, 3502–3508.